

REPORT DOCUMENTATION PAGE

Form Approved
OMB No. 0704-0188

The public reporting burden for this collection of information is estimated to average 1 hour per response, including the time for reviewing instructions, searching existing data sources, gathering and maintaining the data needed, and completing and reviewing the collection of information. Send comments regarding this burden estimate or any other aspect of this collection of information, including suggestions for reducing the burden, to Department of Defense, Washington Headquarters Services, Directorate for Information Operations and Reports (0704-0188), 1215 Jefferson Davis Highway, Suite 1204, Arlington, VA 22202-4302. Respondents should be aware that notwithstanding any other provision of law, no person shall be subject to any penalty for failing to comply with a collection of information if it does not display a currently valid OMB control number.

PLEASE DO NOT RETURN YOUR FORM TO THE ABOVE ADDRESS.

1. REPORT DATE (DD-MM-YYYY) 04-05-2010	2. REPORT TYPE Final	3. DATES COVERED (From - To) From 31-12-2005 To 31-12-2009
--	--------------------------------	--

4. TITLE AND SUBTITLE Experimental Investigation of the Role of Defects in Detonation Sensitivity of Energetic Materials: Development of Techniques for Characterization	5a. CONTRACT NUMBER N/A
	5b. GRANT NUMBER N00014-06-1-0265
	5c. PROGRAM ELEMENT NUMBER

6. AUTHOR(S) Craig J. Eckhardt	5d. PROJECT NUMBER
	5e. TASK NUMBER
	5f. WORK UNIT NUMBER

7. PERFORMING ORGANIZATION NAME(S) AND ADDRESS(ES) University of Nebraska - Lincoln Lincoln, NE 68588	B. PERFORMING ORGANIZATION REPORT NUMBER
--	---

9. SPONSORING/MONITORING AGENCY NAME(S) AND ADDRESS(ES) Office of Naval Research Regional Office - San Diego 4520 Executive Drive, Suite 300 San Diego, CA 92121-3019	10. SPONSOR/MONITOR'S ACRONYM(S)
	11. SPONSOR/MONITOR'S REPORT NUMBER(S)

12. DISTRIBUTION/AVAILABILITY STATEMENT
Approved for Public Release

13. SUPPLEMENTARY NOTES

20100409167

14. ABSTRACT
A final report of the activity related to the research on the role of defects and electronic structure on the sensitivity of energetic materials to detonation.

15. SUBJECT TERMS
RDX, HMX, Brillouin scattering, mechanochemistry, hot spots, insensitive detonation, VUV spectroscopy, defects

16. SECURITY CLASSIFICATION OF:			17. LIMITATION OF ABSTRACT SAR	18. NUMBER OF PAGES 24	19a. NAME OF RESPONSIBLE PERSON Craig J. Eckhardt
a. REPORT UU	b. ABSTRACT UU	c. THIS PAGE UU			19b. TELEPHONE NUMBER (Include area code) 402-489-5132

The PI left for his year of Faculty Developmental Leave in January, 2006 for six months as a visiting professor at the University of Milan. The PI returned in June, 2006. The last five months of the year was spent as a Senior Fulbright Fellow at the Wroclaw University of Technology. The PI applied for, and was granted, the Faculty Leave of Absence and Fulbright Fellowship before the award for this ONR research was announced. Because the departure for Milan was, for practical purposes, at the inception of the grant, the search for postdoctoral associates had to be initiated from abroad. A great deal of time was taken in trying to locate suitable postdoctoral associates over that time. However, few with the necessary background were identified and those that were either had prior commitments or were not interested in pursuing the position due, in no small part, to visa problems. This proved to be quite time-consuming even though unsuccessful. With this, Dr. Goldwasser and I agreed that probably little would be accomplished the first year of the grant and that a no-cost extension at the end of the grant period would have to be executed to allow proper conclusion of the proposed research. However, with the graduation of one of the laboratory graduate students who had worked on energetic materials for his PhD, it appeared that it could be possible to make some progress on the research. The individual, J. J. Haycraft, agreed to work on the project. He began to devise an experimental protocol for measurement and introduction of defects in the energetic materials. The initial work was focused on design and construction of an apparatus for injecting defects into the crystals using PZT ceramics. Unfortunately, Dr. Haycraft was made an extremely good job offer arising from a prior application. He left in August for his new position.

A paper was published by the PI [*Mol. Cryst. Liq. Cryst.* **456** (2006) 1 - 14] wherein a proposed mechanism for detonation was discussed. This publication was a result of the grant support.

During this time, the PI was engaged in working with his collaborator, Prof. Gavezzotti at the University of Milan, on trying to develop a calculational approach to understanding the role of defects in solids of energetic materials. In the course of this work, it was found that the density of crystals of energetic materials are abnormally high compared to crystals of other organic molecular crystals. This was investigated by calculation and it was found that, contrary to commonly held belief, the intermolecular forces in these solids were significantly more strong than the Coulombic interactions. The results of these lattice energy investigations were submitted to the *J. Phys. Chem.* and subsequently published in that Journal. (C. J. Eckhardt, A. Gavezzotti, *J. Phys. Chem. B* **111** (2007) 3430.)

With Dr. Haycraft's departure, the search for the second postdoctoral associate had to be expanded to a search for two associates. Dr. Himansu Mohapatra was hired to continue with the work begun by Dr. Haycraft. In addition, Dr. Mohapatra was charged with the growth of suitable crystals of the less common polymorphs of HMX and RDX. While they could be obtained, they were not of the optical quality needed for the proposed experiments. Dr. Mohapatra spent the bulk of his time in trying to devise suitable methods of growth of the polymorphs of the two energetic materials. The search continued for the second postdoctoral associate. The search focused more on scientists in the US in order to avoid the problems with foreign workers. Further, it became evident that the criteria for the positions would have to be severely modified. This permitted identification of several potential people. One, in particular, was almost perfectly

suiting to the position but declined the offer in favor of another. This pattern repeated. However, Dr. Haidong Zhang, with a new PhD from the University of Florida, agreed to join the group in August, 2007. This was particularly welcome since Dr. Zhang had some familiarity with working at synchrotrons. The light source for the proposed vacuum ultraviolet (VUV) spectroreflectometer is to be the CAMD synchrotron light source in Baton Rouge.

Upon arrival, Dr. Zhang began immediately to work on the design of the VUV spectroreflectometer. This is not a simple task since the sample, an organic, is inherently unstable in a vacuum. Nevertheless, as of December, 2007, Dr. Zhang had made very good progress in identifying the problems inherent with this difficult experiment. By December, 2007, he was identifying what components were viable and had design drawings for the instrument. It is anticipated it will be installed in the summer of 2008. Dr. Zhang's appointment runs to August, 2008 and he has agreed to stay another year to complete the research.

Near the end of 2007, a second postdoctoral associate with experience in Brillouin scattering was identified. Dr. Zhando Utegulov, formerly at NIST, agreed to join the project and work on the defect problem. Dr. Mohapatra had indicated that he would rather have another project and he was able to successfully help Dr. Utegulov move into the defect studies of the proposed research.

Upon return from his leave of absence and Fulbright Fellowship, the PI learned that the entire program under which this research was funded had been cancelled by the new Program Director. Because the PI had not been notified of this action and because there were commitments to the postdoctoral associates who had been hired, the period of the grant was extended with phase out funds so the postdoctoral associates could be allowed time to find positions. The activity during this period focused on completing experiments in progress, closing down instrumentation and disposal of chemicals.

PUBLICATIONS

C. J. Eckhardt, "Mechanochemistry: the last energetic frontier", *Mol. Cryst. Liq. Cryst.* **456** (2006) 1 - 14.

C. J. Eckhardt and A. Gavazzotti, "Computer Simulations and Analysis of Structural and Energetic Features of Some Crystalline Energetic Materials," *J. Phys. Chem. B*, **111** (2007) 3430 - 3437.

3b2 Version Number : 7.51c/W (Jun 11 2001)
File path : p/Santype/Journals/Taylor&Francis/Gmcl/v456n1/gmcl178573/gmcl178573.3d
Date and Time : 22/6/06 and 12:18

Mol. Cryst. Liq. Cryst., Vol. 456, pp. 1–14, 2006
Copyright © Taylor & Francis Group, LLC
ISSN: 1542-1406 print/1563-5287 online
DOI: 10.1080/15421400600786249



Mechanochemistry: The Last Energetic Frontier

Craig J. Eckhardt

Department of Chemistry, Center for Materials Research and Analysis,
University of Nebraska – Lincoln, Lincoln, Nebraska, USA

*A model for the thermal introduction of mechanical energy into electronic degrees- 5
of-freedom of molecules in crystals is discussed. This model is related to the
hypothesis of HOMO-LUMO gap closure for detonation initiation. However, it is
demonstrated that complete gap closure is not required for chemical processes to
occur with the amount of closure related to chemical hardness. A new area of
mechanochemistry can be developed where novel chemistry can be found. It is proposed 10
that the term “mechanochemistry” be limited only to those chemical pro-
cesses that are not driven by the thermalization of the mechanical energy.*

Keywords: chemical hardness; deformation potential; detonation; DSP; mechanochem-
istry; solid-state reaction

INTRODUCTION

15

Why are solid-state reactions of interest? Specifically, why are those of
organic crystals worthy of study? We are, in the main, surrounded by
solid matter and yet the overwhelming amount of study of chemical
processes deals with reactions in solutions. Chemistry in crystals dif- 20
fers significantly from these for solid-state reactions occur in a diffu-
sionless environment. Because of the restrictions of geometry and
the relative orientations of reactants, there is typically a unique reac-
tion pathway leading to specific products. In the case of crystal-to-
crystal reactions, a quantitative yield of a single product is usual. Such
products may not correspond to the high yield products produced by 25
the same reaction in a fluid phase, and may even be of low or no yield

This research was supported by grants from Pfizer, Inc. Critical comments by
Drs. J. J. Haycraft and L. L. Stevens are appreciated.

Address correspondence to Craig J. Eckhardt, Department of Chemistry, Center for
Materials Research and Analysis, University of Nebraska – Lincoln, Lincoln, Nebraska
68588-0304, USA. E-mail: eckhardt@unlserve.unl.edu

theory of solid-state reactivity [2]. The next section will review 70
current concepts used in organic solid-state chemistry to illustrate
how mechanical processes are involved. The 2,5-distyrylpyrazine
(DSP) crystal is used as an example system, exemplifying the role
of mechanical forces in a prototypical crystal-to-crystal organic
solid-state reaction. Next, current mechanochemical models are dis- 75
cussed with emphasis on one that not only accounts for known
phenomena, but also has some predictive power. Another objective
is to present a conceptual, and admittedly heuristic, framework of
the model largely free of mathematical detail but, unfortunately,
with the sacrifice of specificity and clarity that comes with a more 80
quantitative treatment. The paper concludes with discussion of
outcomes of this model.

CONCEPTS FOR ORGANIC SOLID STATE REACTIONS

The statement of the topochemical principle, that “a solid-state reac-
tion will proceed along the path which requires the least amount of 85
movement of the atoms or molecules involved” [3], together with the
corollary that distances between reacting centers should be no greater
than 42 pm, may be regarded as the fundamental phenomenological
rule for solid-state reactivity. Clearly, the postulate carries mechan-
ical implications. Further conceptual expansion was achieved with 90
the suggestion of a reaction cavity: “a region of the crystal surrounding
the reacting species and product” [4]. This could be considered as the
introduction of a defect into the host (reactant) crystal lattice.
Whether this view is chosen or not, the reaction cavity must certainly
be associated with some kind of local mechanical deformation. Actual 95
involvement of the lattice dynamics was suggested by the proposition
of phonon-assisted reactions where “certain collective vibrations
(phonons) of the crystal may coincide with motions along the reaction
coordinate” [5]. This was complemented by the idea of steric compression,
“a force acting at or near the reaction site that influences the 100
atomic motions along the reaction coordinate” [6]. The crucial influ-
ence of local strain on solid-state reactions was demonstrated in a
series of studies on the photodecomposition of peroxides [7]. All of this
work clearly points toward the importance of the role of mechanical
energy in influencing solid-state reactions. 105

These concepts, when coupled with experimental findings, are
qualitative and essentially phenomenological. In order to formulate
a more quantitative picture, the problem must be framed in terms of
the energetics of the system. The fundamental physical question is:
How do the potentials of reactant, product and lattice interact and 110

modify each other during the course of a solid-state reaction when the system is stimulated by mechanical energy?

Thus mechanical properties are intimately involved with the chemical behavior of solid-state reactions. The elastic properties of the reactant crystal are particularly relevant to the intermolecular forces that hold the crystal together and that must be modified during the course of the reaction. It is important to note that these properties arise from collective interactions of the molecules and are not easily associated with a single molecule or even a small cluster of them. These attributes, all associated with the mechanical properties of the crystal, are necessarily implicated when mechanical energy is imparted to the crystal, i.e., the elastic response of a crystal to an external stress must be integral to any mechanochemical event. It is necessary to examine the role mechanical properties play and to identify the non-thermalized mechanism of transfer of mechanical energy from the crystal to the molecules. An important consideration is the assessment of the extent these properties are modified when the crystal is subjected to stress. For simplicity, they are assumed not to change significantly.

MECHANOCHEMICAL MODELS

The previous discussion has shown that mechanical properties are intimately involved with the course of a solid-state reaction. This does not indicate how mechanical energy, which must be mediated by the mechanical properties of the crystal, becomes available for direct molecular excitation.

It is useful to examine those solid-state reactions that are most responsive to mechanical excitation, explosions. When a crystal of an explosive is struck, a shockwave is injected into the solid resulting in detonation. If the mechanism for this process can be found, then it should be generally applicable to other mechanochemical events. The mechanism sought is for the *very initial event* for detonation. Once the process is begun by causing the molecule to break a bond, then the tremendously complicated chemistry and intricate disposition of energy associated with the detonation wave takes hold. However, this does not involve the fundamental question of how mechanical energy is directly introduced into the molecular degrees of freedom.

It is useful to review the physics of the various kinds of chemistry, based on the nature of the source of energy. Figure 1 schematically depicts how thermo-, photo- and electro-chemistry are explained in terms of molecular energetics. In the case of heat, reactivity occurs by exciting the molecule's vibrational manifold. Sufficient heating will lead the molecule's vibrational energy to "climb" to the top of the

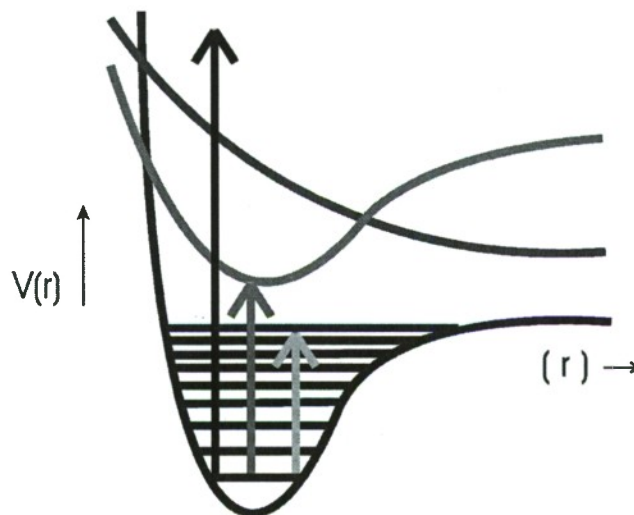


FIGURE 1 Potential energy diagrams showing thermal (short line), photo- (intermediate length line) and electro-chemical processes. A mechanochemical process would drive the system up the repulsive part of the ground state potential.

vibrational ladder and thus dissociate. In photochemistry, a photon excites the molecule to an excited state, and it is that state that suffers chemical reaction. It is more difficult to depict electrochemical events with such a simple diagram but, crudely, it may be envisaged as a process involving the removal of an electron(s) from the HOMO (or other bonding orbital) or insertion of an electron into the LUMO. 155

But what happens when mechanical stress is applied? Of course, it must be applied to a ponderable body and not to an individual molecule. Nevertheless, the energy must enter the molecular degrees of freedom in some way. An appealing approach has been proposed whereby the energy of the shockwave is absorbed by the “phonon bath” of the crystal [8]. These excited lattice vibrations are pumped to high populations by the extreme compression of the shock wave. A molecule with sufficiently anharmonic, low-frequency, vibrational modes, termed “doorway modes,” that are approximately twice the frequency of the phonon fundamentals, can then couple with the phonons. This would allow the energy to flow into the vibrational modes of the molecule. At this point, the process would then be the “ladder climbing” associated with thermochemical reactions. The model is, essentially, a thermalization of the mechanical energy. The model quite elegantly addresses the most common case of degradation of mechanical energy to heat. 160 165 170

However, it takes less than 100 femtoseconds for the shockwave to traverse a molecule, a time too short for slow thermalization processes. Only excitation of electrons is sufficiently fast to respond and to absorb the large amount of power associated with the shockwave. Gilman [9] pointed out that closure of a molecule's HOMO-LUMO gap could be induced by mechanical shear, a condition consistent with a shockwave. When this gap closes the electrons become delocalized leading to "metallization." The resulting "plasma" is unstable when the shockwave passes and thus leads to detonation.

It has been shown that some products of detonation are the same as those found from photodecomposition of the energetic material [10] and that the products, especially at the outset, are not undifferentiated. Thus, a model must be found that provides for this observation, a difficulty for a metallized system. Based on the concept of chemical pressure and a previously proposed model for solid-state reactivity, Luty, Ordon and Eckhardt have formulated a model that is consistent with all observations.

Study of Figure 1 readily leads to understanding the basic concept that is a generalization of the HOMO-LUMO gap closing previously proposed. When suffering the extreme compression of a shockwave, the close-packed molecules of the crystal are forced against each other such that they undergo some kind of shear. This will involve compression. This forces movement up the repulsive part of the potential, a region of the potential rarely considered by chemists. Since this segment of the potential is bound, the energy of the molecule increases rapidly with compression until there is intersection with the potential energy surface of a higher energy state. At this point, the two intersecting states must mix.

The first-order model considers only mixing of the HOMO and LUMO. This leads to a *distortion-induced molecular electronic degeneracy* (DIMED) that produces what may be regarded as a new ground state that is consistent with the molecule's response to the shockwave. The process involves both inter- and intra-molecular transfer of electrons. The resulting instability leads to chemical reaction. It should be emphasized that this will occur before metallization, i.e., before complete closure of the HOMO-LUMO gap. The point at which this occurs depends upon the specific material. Conceptually, the situation parallels that of kinetic theory for electron transfer reactions.

The Example of 2,5-distyrylpyrazine

The solid-state, crystal-to-crystal photoreaction of DSP, a readily polymerizable molecule in solution, is a well-studied system that

exemplifies many of these concepts [11]. Further, it shows the role of strain and defects in the solid-state reaction. Initial studies showed that the DSP crystal's products were dependent upon the frequency of the exciting light. High polymer is obtained when light of frequencies greater than 25 kK (1 Kayser = 1 cm^{-1}) irradiates the sample whereas at lower frequencies only oligomers are obtained. This has been explained by an excitonic mechanism wherein highly localized $\pi^* \leftarrow n$ excitons [12], which are only created at frequencies below 25 kK, lead to production of oligomers. At higher photon energies, delocalized $\pi^* \leftarrow \pi$ excitons, essentially excitation energy that can travel through the lattice, are able to continually "feed" energy for the growth to higher molecular weight polymers. The growth is only stopped when the $\pi^* \leftarrow \pi$ excitons fall into traps in the crystal such as defects. Thus, the solid-state reaction is driven by direct excitation of the reactant crystal by electromagnetic radiation.

Mechanical properties mediate the lattice, and it has been shown through following the frequencies and intensities of the Raman-active DSP lattice modes as a function of extent of reaction, that the elastic properties of the host (reactant) lattice determine when the transformation from the reactant to the product crystal occurs. In the case of DSP crystals, this transformation occurs at a fairly high conversion of 65%. The conversion is driven by the build-up of local strain fields around the product molecules. As the number of product molecules increases and the surrounding strain fields increase, a point is reached where the local strain fields couple and drive the transformation to the product lattice. This is the point where the elastic limit of the reactant lattice is exceeded, and it can no longer retain itself. Of course, in many solid-state reactions the strain can be so severe that it causes destruction of the crystal lattice. This picture complements the previous strain studies and demonstrates that both the reaction cavity and steric compression are concepts that fit within the strain field and its development during the course of a reaction in a crystal. The salient point is that the elastic properties of the reactant lattice "control" the reaction pathway and it may be expected that, if possible, products will grow into the more compliant regions of the lattice. However, the product lattice may also be generated from large, cooperative motions of the reacting species.

Depending upon the elastic behavior of the surrounding lattice these forces will vary according to the resistance that is met. This resistance and its magnitude, may be identified with steric compression. Both of these can be seen to be aspects of a more general quantity, the chemical pressure [13], that may be quantified. Thus, the elastic properties of the reactant lattice strongly influence the

nature of the reaction in the solid. If the parent crystal is softer in one direction than another, this may be expected to influence the ease with which product is formed and the orientation it may adopt.

The local strain fields about product molecules will be isolated at small product concentrations, but as the amount of product builds, the strain fields are no longer isolated and they will couple. This coupling will drive the system to the daughter lattice. However, depending upon the potential energy surface of the latter, shattering of the crystal during the course of the reaction may be observed because of incommensurate lattice parameters. In fact, this is usually the most common fate of solid-state reactions.

This demonstrates the importance of the role of mechanical properties in a solid-state reaction. The energetics certainly arise from the mechanical properties of the crystal, but their role is quite different from the question of direct conversion of mechanical energy to chemical degrees of freedom. The mechanical interactions described by the DSP solid-state reaction do not involve the internal modes of vibration or electron distribution in the molecule. In fact, it is the photonic energy that drives the process by direct excitation of the molecules and not mechanical energy. The mechanical processes in the solid-state reaction are responsive to the generation of product and are not initiatory. Investigation of this requires a model that details the fate of the mechanical energy that is introduced into the lattice.

THE MECHANOCHEMICAL MODEL AND MOLECULAR HARDNESS

The application of mechanical energy is most often achieved by application of stress, usually compression, to the crystal. To involve the molecular degrees of freedom, Gilman has pointed out that it is necessary to have shear stress since hydrostatic stress is not expected to significantly affect the geometry of the molecule, save through decreasing its size. When driven up the *bound* repulsive part of the potential, an intersection with a higher energy state will eventually occur. When this happens, mixing of the ground state potential and that of the upper state will occur. Depending upon how steep the repulsive part of the potential is, there may be nearly simultaneous mixing between several states. However, consideration is restricted to the simple two-state situation, specifically mixing that involves HOMO-LUMO mixing.

This is an *electronic* process since only electronic states are capable of response on the timescale of the shockwave and are able to provide absorption of the large energies involved. Further deliberation leads to the conclusion that the governing condition is not the timescale of the

mechanical event, but rather, the amount of mechanical power that must be accommodated. When the power is low, then thermalization is the expected process but when it is high, the vibrational modes cannot store the available energy efficiently and only the electronic modes would have that capacity. It is the latter that is of chemical interest. 300

Molecular hardness, η , measures a molecule's resistance to electronic change [14]. It is defined by:

$$\eta = \frac{1}{2}[I - A]$$

where I is the ionization potential and A the electron affinity. This is relevant because a change in the electronic distribution must be associated with the high mechanochemical power. Hardness' importance arises because it is tied to both the deformation of the molecule as well as to how the molecule packs in the crystal. 310

The specific mechanochemical reaction of detonation initiation has been used to guide thinking about mechanical energy into molecular degrees of freedom, but the mechanism need not be specific to this type of reaction. Whatever chemistry may arise, it will be associated with the deformation-induced state mixing that leads to the decrease of the HOMO-LUMO gap. It is expected that different higher energy electronic states will mix differently, since they will have different electronic distributions. 315

In the simple model under consideration, deformation leads to the closure of the HOMO-LUMO gap. As the gap decreases, the state mixing may be expected to increase. Alternatively, as the hardness decreases, the mixing will become greater. Thus, for the "metallization" model, $\eta \rightarrow 0$. But is complete HOMO-LUMO gap closure necessary for a chemical reaction, or for detonation initiation in particular? Q1 320

To address this, knowledge is required of how the change in energy on closure of the gap is related to the molecular hardness. The process can be envisaged as a sequence beginning with an initial distortion due to the stress that affects the electronic energy of the molecule and thus alters its hardness. The change of the hardness must lead to a change in the energy of the HOMO-LUMO gap that leads to state mixing and a new set of states. Complete closure is not required, but rather, a critical deformation must occur wherein the new potential surfaces develop. The resultant lower energy potential surface can be viewed as the compressional "ground state" (CGS) that is found at some critical value of the HOMO-LUMO gap closure. 325 330

In the case of detonation initiation, the higher energy state that is mixing is either dissociative or leads to dissociative character in the CGS. This is illustrated in Figure 2, where it is shown that some 335

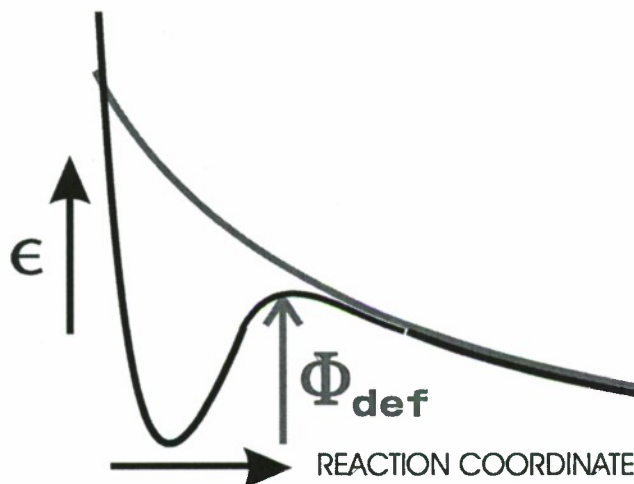


FIGURE 2 A “kinetic” plot showing the CBS (dark line) resulting from the mixture of the unstressed ground state and a dissociative excited state (light line). The role of the deformation potential in achieving detonation is shown.

critical deformation energy exists that allows the system to overcome the barrier between the bound portion of the potential and the dissociative tail. Once overcome, detonation initiation will ensue. However, if the CGS arises from mixing of two bound states, then the CGS itself should, because it differs from the two mixing states, produce new chemistry much akin to the photochemical products produced by photo-excited states. This holds promise for a new area of solid-state chemistry.

Another way of thinking about this phenomenon is to envisage the reverse process where photoexcitation to an excited state of a molecule creates a deformation of both the molecule and its surroundings. The electronic relaxation channels into vibrational degrees of freedom. The coupling that leads to this will be the same coupling that would lead to a molecular excitation by a mechanically-induced deformation at the site. A deformation energy, Φ_{def} , can be defined for a lattice that is perturbed by compression. The energy change arising from m such perturbed molecules is $\Delta E = mE_0 + \Phi_{\text{def}}$. The amount of deformation required to *promote* an electron from the HOMO to the LUMO is $E_0 = \Phi_{\text{def}}$ allowing for the fact that, while in a crystal, the HOMO and LUMO are bands which are quite narrow for molecular crystals. Their energies may then be taken as equivalent to the molecular values which leads to $E_0 = I - A = \Phi_{\text{def}}$. This is the condition for the electronic instability of the lattice toward deformation and it can be seen that $\Phi_{\text{def}} = 2\eta$.

This molecular deformation that is associated with the promotion of the HOMO electron to the LUMO can be determined from the condition for a minimum of the total molecular energy. This allows another expression for the hardness:

365

$$\eta = \eta_0 - \frac{1}{2} \sum_x k_x \langle Q_x \rangle^2$$

where normal coordinates, Q_x , with force constants, k_x , are used to describe the deformation.

How is the molecule affected by deformation? The undeformed molecule will have a chemical potential, $\mu_0 = 1/2(I + A)$, and a hardness, $\eta_0 = 1/2(I + A)$. The molecular energy must change upon its deformation, which is reflected in the change in the number of electrons in the frontier orbitals, ΔN :

$$\Delta E = \mu (\Delta N) + \eta (\Delta N)^2 + \frac{1}{2} \sum_x k_x \langle Q_x \rangle^2$$

Because of the deformation, the chemical potential will change:

375

$$-\left(\frac{\partial \mu}{\partial Q_x}\right)_N = \varphi_x$$

as will the molecular hardness:

$$\eta = \eta_0 - \frac{1}{2} \sum_x \frac{\varphi_x^2}{k_x}$$

Modes that describe the molecular deformation will contribute most to the diminution of the molecular hardness.

380

Q1 It has been shown that the instability condition $\eta \leq 0$ provides the criterion for the critical distortion necessary for the *mechanochemical* promotion of an electron from the HOMO to the LUMO:

$$\sum_x k_x \langle Q_x \rangle_{\text{crit}}^2 = (I - A)$$

This promotion can occur before complete closing of the HOMO-LUMO gap leading to a DIMED. It may be viewed as an "inverse" Jahn-Teller effect because its creation is due to structurally relaxed electronic states.

385

Since hydrostatic stress nominally affects the gap closing, the deformation is due to an imposed shear stress that raises the molecule's potential energy from the bottom of the potential to the deformation energy, Φ_{def} . The electrons will immediately rearrange according to the deformation with subsequent vertical relaxation to a new state

390

where the molecule is deformed with an electron in its HOMO and one in its LUMO. If the minimum of the potential well of the new DIMED-
formed CGS is above the energy of a reactant, relaxation will return
the molecule to the reactant state. This will happen when the deformation
that occurs cannot compensate for the expense of electronic energy, i.e., $(I - A) > \Phi_{\text{def}}$. However, such relaxation will not occur
when the molecule is critically deformed where the molecular state
has equally occupied HOMO and LUMO, a condition which is stable.
The critical deformation is necessary for the HOMO-LUMO gap "closure."
At this point, there will be an electronic energy level with a width
designated as $2t$ and a population of 0.5. An insufficient deformation of
the molecule forms a non-relaxed HOMO-LUMO degeneracy. Extra
deformation energy is required, however, to stabilize the system for
it may relax to the unstressed ground state. The energy required to
stabilize the CGS must be supplied by cooperative interactions. If
 $(I - A) < \Phi_{\text{def}}$ then there will be spontaneous creation of CGS molecules.
It is these that can do chemistry.

IMPLICATIONS

Mechanochemistry and solid-state chemistry must be synonymous since only solids can suffer shear stress. While most mechanical energy is thermalized and the chemistry that ensues is based on the fate of heat in a chemical process, the direct effect on molecular
degrees of freedom by mechanical energy, which will likely be due to
compressive forces, may be expected to generate new chemistry.

The simplest process that may be associated with this model is the generation of light when a substance is compressed. Common triboluminescence is attributed to excitation of ambient gas molecules to emit
in the presence of high fields created by fissures in crystals. However, another "anomalous" triboluminescence does not correlate with the emission of the ambient gas but apparently inheres in the substance itself. It has been argued that this arises from differences in calibration of instruments, self-absorption or fracture-induced perturbations.
However, while the first explanation is certainly independent of the substance and the second is correctable, the third clearly relates to the mechanical properties of the material and may well arise from mechanical excitation to form a CGS which would be capable of emission that differs from the normal excited state of the uncompressed
molecule. The local stresses developed by fracture are consistent with a mechanochemical process. The common observation of light emitted from detonating material is also consistent with the mechanochemical model.

Detonation initiation itself is the most obvious example of a 435
mechanochemical process. Because molecules must have higher
energy dissociative potentials, there should always be a shear com-
pression of sufficient magnitude to cause mechanochemical mixing
of the ground state with a dissociative one. The prediction is that there
will always be a sufficiently large compression that involves shear that 440
will cause detonation. Thus, barring another process that may cause
disintegration of a substance, detonation should always be possible
for any material. Reported research on compressively induced detona-
tion of non-energetic materials substantiates this [15]. Even if a
stable CGS is created, detonation is a likely event if the system is near 445
the critical deformation energy since but a slight decrease of com-
pression would create an unstable situation and the sudden relaxation
to the original state could also be destructive.

More productive from the chemist's viewpoint is the possibility of
new chemistry. The CGS is a molecular state that is capable of doing 450
chemistry. It certainly differs from the parent states and suggests that
heretofore unexplored chemistry may be available. Just as photochem-
istry is dictated by the nature of the excited state of a molecule,
mechanochemistry will be dictated by the peculiarities of the CGS.
The recently developed capability to grow binary crystals [16] suggests 455
that mechanochemical reactions that are other than unimolecular are
within reach. However, even study of the reactions of single compo-
nent crystals may be expected to be fruitful and, combined with DFT
calculations, may produce a new area of chemical study.

REFERENCES

460

- [1] Luty, T., Ordon, P., & Eckhardt, C. J. (2002). *J. Chem. Phys.*, *117*, 1775.
- [2] Luty, T. & Eckhardt, C. J. (1995). *J. Amer. Chem. Soc.*, *117*, 2441.
- Q2 [3] Cohen, M. D. & Schmidt, G. M. J. (1964). *J. Chem. Soc.*, 1996.
- [4] Cohen, M. D. (1975). *Angew. Chem. Int. Ed.*, *14*, 386.
- [5] Prasad, P. N. & Dwaradanath, K. (1980). *J. Amer. Chem. Soc.*, *102*, 4254. 465
- [6] McBride, J. M. (1983). *Accts. Chem. Res.*, *16*, 304–312; Ariel, S., Askari, S., Scheffer, J. R., Trotter, J., & Walsh, L. (1985). In: *Organic Phototransformations in Nonhomogenous Media*, Fox, M. A. (Ed.), ACS Symposium Series No. 278: 243–256.
- [7] McBride, J. M. (1983). *Mol. Cryst. Liq. Cryst.*, *96*, 19; *ibid.* (1983). *Acct. Chem. Res.*, *16*, 304; Hollingsworth, M. D. & McBride, J. M. (1989). *Adv. in Photochem.*, *15*, 279. 470
- [8] Dlott, D. D. & Fayer, M. D. (1990). *J. Chem. Phys.*, *92*, 3798; Kim, H. & Dlott, D. D. (1990). *J. Chem. Phys.*, *93*, 1695; Tokmakoff, A., Fayer, M. D., & Dlott, D. D. (1993). *J. Phys. Chem.*, *97*, 1901.
- [9] Gilman, J. J. (2003). *Mater. Res. Soc. Symp. Proc.*, *800*, 287; *ibid.* (2001). *Chem. Electrochem. Corros. Stress Corros. Cracking*, Proc. Symp., Jones, R. H. (Ed.), 475
Minerals, Metals & Materials Society, Warrendale, PA, 3–25; *ibid.* (2000). *AIP Conf. Proc.*, *505*, 809; *ibid.* (1999). *Mater. Res. Soc. Symp. Proc.*, *539*, 145; *ibid.*

- (1999). *Phil. Mag.*, *B79*, 643; *ibid.* (1998). *AIP Conf. Proc.*, *429*, 313; (1997). *Mater. Res. Soc. Symp. Proc.*, *453*, 227; *ibid.* (1996). *Science*, *274*, 65; (1995). *AIP Conf. Proc.*, *370*, 215; *ibid.* (1995). *Phil. Mag.*, *B77*, 1057; *ibid.* (1994). *AIP Conf. Proc.* 480 *309*, 1349; Gilman, J. J. & Armstrong, R. W. (1994). *AIP Conf. Proc.*, *309*, 199;
- Q3 Gilman, J. J. (1992). *Mater. Res. Soc. Symp. Proc.*, *276*, 191; *ibid.* (1993). *Phil. Mag.*, *B67* ■; *ibid.* (1992). *J. Mater. Res.*, *7*, 535.
- [10] Im, H.-S. & Bernstein, E. S. (2000). *J. Chem. Phys.*, *113*, 7911.
- [11] Hasegawa, M. (1995). *Adv. Phys. Org. Chem.*, *30*, 117; Zeng, Q., Wang, C., Chen, B., 485
Chunli, L., Li, Y., & Yan, X. (1999). *J. Vac. Sci. Tech.*, *B17*, 2447; Takahashi, S.,
Miura, H., Kasai, H., Okada, S., Oikawa, H., & Nakanishi, H. (2002). *J. Amer. Chem. Soc.*, *124*, 10944.
- [12] Peachey, N. M. & Eckhardt, C. J. (1993). *J. Amer. Chem. Soc.*, *115*, 3519; *ibid.* 490
(1992). *Chem. Phys. Lett.*, *188*, 462; *ibid.* (1993). *J. Phys. Chem.*, *97*, 10849.
- [13] Luty, T. & Fouret, R. (1989). *J. Chem. Phys.*, *90*, 5696.
- [14] Pearson, R. G. (1997). *Chemical Hardness*, Wiley-VCH: Weinheim.
- [15] Enikolopyan, N. S., Aleksandrov, A. I., Gasparyan, E. E., Shelobkov, V. I., &
Mkhitarian, A. A. (1991). *Doklady Akad. NAUK*, *319*, 612; Enikolopyan, N. S.,
Mkhitarian, A. A., Karagezyan, A. S., & Khzardzhyan, A. A. (1987). *Doklady Akad.* 495
NAUK, *292*, 121.
- [16] Gao, X., Friscic, T., & MacGillivray, L. R. (2004). *Angew. Chem. Int. Ed.*, *43*, 232;
Chu, Q., Swenson, D. C., & MacGillivray, L. R. *ibid.* (2005). *44*, 3569.

Computer Simulations and Analysis of Structural and Energetic Features of Some Crystalline Energetic Materials

Craig J. Eckhardt*

Department of Chemistry, University of Nebraska—Lincoln, Lincoln, Nebraska 68588-0304

Angelo Gavezzotti*

Dipartimento di Chimica Strutturale e Stereochimica Inorganica, Università di Milano, Via Venezian 21, 20133 Milan, Italy

Received: October 23, 2006; In Final Form: January 23, 2007

A database of 43 literature X-ray crystal structure determinations for compounds with known, or possible, energetic properties has been collected along with some sublimation enthalpies. A statistical study of these crystal structures, when compared to a sample of general organic crystals, reveals a population of anomalously short intermolecular oxygen–oxygen separations with an average crystal packing coefficient of 0.77 that differs significantly from 0.70 found for the general population. For the calculation of lattice energies, three atom–atom potential energy schemes and the semiempirical SCDS-PIXEL scheme are compared. The nature of the packing forces in these energetic materials is further analyzed by a study of the dispersive versus Coulombic contributions to overall lattice energies and to molecule–molecule energies in pairs of near neighbors in the crystals, a partitioning made possible by the unique features of the SCDS-PIXEL scheme. It is shown that dispersion forces are stronger than Coulombic forces, contrary to common belief. The low abundance of hydrogen atoms in these molecules, the close oxygen–oxygen contacts, and the high packing coefficients explain the observation that, for these energetic materials, crystal densities are anomalously high compared to those of most organic materials. However, an understanding, not to mention prediction or control, of the deeper mechanisms for the explosive power of these crystalline materials, such as the role of lattice defects, remains beyond present capabilities.

I. Introduction

Weighing the advantages and dangers of developing more efficient energetic materials is a difficult matter that involves ethics and politics rather than pure science, but it requires due consideration of the fact that the preponderant use of explosives is for non-military applications. There are two overriding concerns for those who use these materials: safety and explosive power. Energetic materials that are resistant to detonation can be handled more safely, although often at the expense of explosive power. These matters are amenable to the usual studies of structure–property relationships, hence the present work.

For decades, explosive power has been correlated with the energy density of the material and, in particular, with the mass density because of the dependence of the magnitude of the detonation velocity and of the detonation sensitivity to this simple physical property.¹ For crystals comprised only of atoms of elements of the first and second periods, the densities of energetic materials tend to be anomalously large. This may have implications regarding defects, since they usually lower the density. Another important measure of explosive power has been the oxygen balance that is taken to be optimal when the amount of oxygen in the energetic material is just sufficient for conversion of all oxygen to only carbon dioxide and water.²

Most energetic materials are organic molecules of rather irregular shape, and thus a question of interest is how these

molecules pack in crystals to obtain the most efficient space occupation and hence a high density for a given chemical composition. For such oxygen-rich substances, it would normally be expected that closely packed molecules that have many peripheral oxygen atoms would find difficulty in avoiding close and, presumably, repulsive contacts. A crucial matter then is the nature and magnitude of the intermolecular forces that bind the molecules in these crystals. A related topic is crystal polymorphism, because different polymorphs exhibit varying sensitivity to detonation, thus confirming that solid-state properties must have significant influence on the mechanism of detonation.^{1a} A proper understanding of crystal packing forces may help in controlling the growth of favorable polymorphs. Further, the study of “perfect” crystals is a first step in the analysis of the defects which disrupt the crystal lattice and presumably have a significant influence on the performance of these materials.³

For these reasons, we have undertaken a detailed packing analysis and examination of the binding forces of a series of crystals of energetic materials by a combination of recently developed statistical techniques and molecular simulation methods.⁴ Using crystallographic databases, some geometrical features of the crystal packing of energetic materials are compared with those of a general collection of organic compounds. For the calculation of intermolecular energies, the available empirical atom–atom force fields are critically examined, but the results are also compared with those obtained by more accurate semiempirical and *ab initio* methods. The

* Authors to whom correspondence should be addressed.

prospects for an accurate and reliable simulation of these materials are then examined.

II. Experimental Data

1. Heats of Sublimation. The sublimation enthalpy, ΔH_{sub} , is a vital piece of information in crystal-structure analysis and force-field calibrations, because its negative should be equal to the calculated lattice energy. The NIST thermodynamic database⁵ was searched for thermodynamic properties of the crystalline materials of interest here, in particular for sublimation enthalpies of compounds whose crystal structure also has been determined by X-ray diffraction. The primary literature⁶ was also searched independently, and often checked to help in making a choice between different ΔH_{sub} values stored in the NIST database. In particular, the ΔH_{sub} for HMX (1,3,5,7-tetranitro-1,3,5,7-tetraazacyclooctane, refcode OCHTET) has been assessed from a Clausius-Clapeyron treatment of the original data.^{6c} The reliability of thermochemical data is somewhat variable, and discrepancies of up to 20–30% among different values for ΔH_{sub} of the same crystal are quite common (for an extreme instance, the reported ΔH_{sub} 's for dimethylnitramine range from 41 to 70 kJ mol⁻¹). The experimental data come from different techniques, or often refer to high temperature, as is appropriate for the measurement of vapor pressures of nonvolatile compounds, while calculated lattice energies derive from structures determined at room temperature. Assuming a typical range of values for gas-crystal ΔC_p 's for organic crystals of 20–40 J K⁻¹ mol⁻¹, one can estimate a 2–4 kJ mol⁻¹ increase in the ΔH_{sub} for a 100 K lowering of the temperature. In view of the inherent uncertainties, the comparison between experimental ΔH_{sub} 's and calculated lattice energies is no more than a guideline in the calibration of crystal potentials, and only an overall consideration of trends over many data can be significant; parametrization based on only a few experimental data can sometimes be misleading.

2. Crystal Structures. The Cambridge Structural Database⁷ (CSD) and the primary literature were searched for X-ray crystal structure determinations of materials with promise for high-energy content, especially molecules containing several nitro groups. The final database of 43 selected crystals (see Tables 1 and 2) is representative rather than exhaustive, but proved to be sufficient for the present purposes. The crystal structure determinations are of variable accuracy as a consequence of changeable crystal quality and the other usual experimental limitations of the X-ray work. This hardly affects the atom–atom force-field calculations, whose potentials are isotropic and radial, and rather insensitive to minor structural variations. However, even a minor inaccuracy in atomic positions significantly affects the ab initio quantum chemical calculations or the PIXEL calculations (see below) that take into account all of the electron density distribution and are much more sensitive to structural details. For example, unrealistic intramolecular energy differences are calculated ab initio for the same molecule extracted from different crystal structure determinations because of geometrical distortions due to different accuracies in atomic positional parameters, which, however small, have large consequences for the intramolecular binding geometry. The effect is less pronounced with intermolecular energies.

III. Statistical and Theoretical Methods

1. Atom–Atom Contact Distributions. The structural database of Table 1 was used to analyze atom–atom contact densities. Distance distribution functions (DDF) are defined as follows:⁸ All atom–atom distances between atomic species i

TABLE 1: Compound Designator Key: Cambridge Structural Database REFCODE, Explosive Acronym (if Extant), and Common Chemical Name

CATJIQ	1,3,3,5,7,7-hexanitro-1,5-diazacyclo-octane
CIWMEA	TNAZ, 1,3,3-trinitroazetidine
CTMTNA	RDX, cyclotrimethylene-trinitramine
DATNBZ	1,3,5-trinitro-2,4-diaminobenzene
DIMNAN	N,N-dimethyl-4-nitroaniline
DNBENZ	1,3-dinitrobenzene
DNITBZ	1,4-dinitrobenzene
DNPMTA	dinitrophenylmethyltetramine
GEMZAZ	1,4-dinitroglucuril
GIMBOT	2,2,4,4,6,6-hexanitrostilbene
HIHHAH	3-nitrobenzaldehyde
JEDSUG	1,3-dinitro-1,3-diazacyclopentane-2-one
JEHLAJ	2,5,7,9-tetranitro-8-oxo-2,5,7,9-tetra-azabicyclo(4.3.0)nonane
JEXLUT	cis-1,3,5,7-tetranitro-1,3,5,7-tetra-azadecalin
JEXMAA	TNBI 1,1,3,3-Tetranitro-4,4-bi-imidazolidine
JEXMEE	TNSD, 1,3,7,9-Tetranitro-1,3,7,9-tetra-azaspiro(4.5)decane
JEXMII	trans-1,4,5,8-tetranitro-1,4,5,8-tetra-azadecalin
KEMTIF	2,4,8,10-tetranitro-2,4,8,10-tetra-azaspiro(5.5)undecane
KOFKAR	1,3-dinitro-1,3-diazacyclohexane
KOFKEV	1,3-dinitro-1,3-diazacycloheptane
KOFKIZ	1,5-dinitro-3-nitroso-1,3,5-triazacycloheptane
METNAM	N,N-dimethylnitramine
MTNANL	TETRYL, 2,4,6-trinitro-N-methyl-N-nitroaniline
MNTDMA	N,N-dimethyl-3-nitroaniline
NACPON	N,N-dimethyl-4-nitroaniline
NITOLU	4-nitrotoluene
OCHTET	HMX, 1,3,5,7-tetranitro-1,3,5,7-tetra-azacyclo-octane
NOHTAZ	2,4,6-trimethyl-1,3,5-trinitrohexahydro-1,3,5-triazine
PUBMUU	HNIW 2,4,6,8,10,12-hexanitro-2,4,6,8,10,12-hexa-azatetracyclododecane, hexanitrohexa-azaisowurtzitane
SECVOL	2,2-bis(1,3-dinitrohexahydropyrimidine)
TATNBZ	1,3,5-triamino-2,4,6-trinitrobenzene
TNBENZ	1,3,5-trinitrobenzene
TNIOAN	1,3,5-trinitroaniline
TNOXYL	1,3,5-trinitro-2,4-dimethylbenzene
TNPHNT	1-ethoxy-2,4,6-trinitrobenzene
ZZZFYW	1,2-dinitrobenzene
ZZZMUC	2,4,6-trinitrotoluene
ZZZQSC	2,4-dinitrotoluene

and j in all crystal structures in the database are calculated up to a certain limit R_{max} . Let $N_k(R)^j$ be the number of atom–atom distances within the k th distance bin between R_k and $R_k + dR$. An inspection of the unnormalized distribution function reveals a separation below which no contacts are observed, R^{oj} . The normalization factor, F_N , and the DDF are then

$$F_{N,ij} = \sum N_k(R)^j / [4\pi/3((R_{\text{max}})^3 - (R^{oj})^3)]$$

$$\text{DDF} = g_k(R)^j = (1/F_{N,ij})N_k(R)^j/dV_k$$

where dV_k is the volume of the spherical shell. F_N represents the condition of uniform distribution of the observed contacts over the available contact space. The DDF is formally similar to a radial distribution function, RDF, but the physicochemical meaning is different, because a RDF refers to a sampling over the same molecular species in a homogeneous system, while the DDF refers to sampling over different molecules and over many different systems, the crystal structures.

2. Ab Initio Calculations. Quantum chemical calculations on isolated molecules with a fixed geometry as extracted from the crystal structure determination were carried out using the GAUSSIAN package,⁹ at the MP2 6-31G** level with the “cube” option to produce an electron density for PIXEL (step of 0.08 Å), and the “pop = esp” option for the calculation of

TABLE 2: Crystal Lattice Energies (kJ mol⁻¹)

CSD refcode	-E(UNI) ^a	ΔH(subl) ^b	-E(PIXEL) ^c	-E(SRT) ^d	E(coul+pol) ^e	E(disp) ^f
CATJIQ	152			183		
CIWMEA	93		84	113	-61	-92
CTMTNA	109	112	116	130	-87	-97
DATNBZ	154	140	116		-75	-121
DIMNAN	108	103	105		-60	-118
DNBENZ	101	85	80		-40	-77
DNITBZ	105	96	89		-49	-80
DNPMTA	130		130	141	-87	-107
GEMZAZ	148		155		-157	-125
GIMBOT	205	180				
HHHHAH	101	110	88		-49	-85
JEDSUG	93		112	124	-86	-81
JEHLAJ	136			181		
JEXLUT	159			179		
JEXMAA	154			176		
JEXMEE	147			173		
JEXMII	155			169		
KEMTIF	160			184		
KOFKAR	101		101	117	-68	-82
KOFKEV	108		106	120	-67	-92
KOFKIZ	117			131		
METNAM	59	70	72	70	-41	-56
MTNANL	134	134	118	150	-77	-106
MNTDMA	104	93	94		-49	-105
NACPON	100					
NITOLU	86	79	71		-30	-73
NOHTAZ	127			141		
OCHTET00	127			179		
OCHTET03	124			168		
OCHTET12	146	162	157	180	-91	-127
PUBMUU00	156			175		
PUBMUU01	165			181		
PUBMUU02	158			187		
SECVOL	152			188		
TATNBZ	190	168	156		-113	-137
TNBENZ10	105	107				
TNBENZ13	107	107	86		-54	-94
TNIOAN	132	120	100		-62	-97
TNOXYL	132	130	103		-58	-104
TNPHNT	119	121	104		-63	-100
ZZZFYW	101	87	88		-46	-76
ZZZMUC	119	105				
ZZZQSC	108	98	89		-46	-91

^a Lattice energy with UNI atom-atom force field.¹¹ ^b Heats of sublimation. ^c Total PIXEL lattice energy. ^d Lattice energy reported in ref 17, with atomic charges from highest-level quantum chemical calculation. ^e Sum of Coulombic and polarization PIXEL terms. ^f PIXEL dispersion energy.

electrostatic-potential-derived atomic point charges. Alternatively, these were also calculated by the so-called rescaled-EHT method,¹⁰ based on a Mulliken population analysis on an Extended Hückel calculation with modified valence-orbital ionization potentials. This produces atomic point charges very similar to those from a Mulliken population analysis on the MP2 wavefunction, and can be routinely applied even to very large molecular systems because of the virtually null computational requirements of an EHT calculation versus a full molecular orbital MP2 calculation. These atomic point charges were used only for the calculation of cell dipoles in the convergence correction, or for comparison with PIXEL Coulombic energies which include penetration energies (see below).

3. Lattice Energies and Molecule-Molecule Energies. Crystal structures were taken as is from the X-ray diffraction determination without optimization of lattice energies or structure relaxation, but hydrogen atom positions were recalculated as usual.¹⁰ Force-field calculations were carried out in the atom-atom approximation with the chargeless UNI force field,¹⁰ which uses a simple $A \exp(-BR) - CR^{-6}$ functional form in the atom-atom distance R . Point-charge Coulombic terms were then evaluated separately using atomic point-charge parameters obtained as described above. For more accurate

calculations, the SCDS-PIXEL approach¹¹ was applied. The molecular electron density is first calculated by standard quantum-chemical methods giving the electron distribution on a large number (10 000–20 000 for our molecules) of charge pixels. The Coulombic energy is then calculated by sums over pixel-pixel, pixel-nucleus, and nucleus-nucleus Coulombic terms. A local polarizability is then assigned to each pixel, the electric field generated by pixels and nuclei in surrounding molecules is calculated, and the linear polarization energy is evaluated. An empirical damping function, using one disposable parameter, is introduced to avoid singularities. The overlap between molecular densities is calculated, and the exchange repulsion energy is evaluated as proportional to the overlap integral. Dispersion energies between two molecules A and B are calculated as a sum of pixel-pixel terms in a London-type expression involving the above-defined distributed polarizabilities and an “oscillator strength” energy, E_{OS} :

$$E_{DISP,AB} = (-3/4) \sum_{i,A} \sum_{j,B} E_{OS} f(R) \alpha_i \alpha_j / [(4\pi\epsilon^0)^2 (R_{ij})^6]$$

where the damping function is $f(R) = \exp[-(D/R_{ij} - 1)^2]$ (for $R_{ij} < D$), where D is an adjustable empirical parameter. Standard

PIXEL theory uses $D = 3.0 \text{ \AA}$, but a preliminary survey showed that all lattice energies of crystals considered here were underestimated with respect to the ΔH_{sub} . Since the parameter is fully adjustable and the effect is systematic, a correction of this parameter to reduce the discrepancy was considered acceptable. $D = 2.6 \text{ \AA}$ is used here, which increases the calculated dispersion energies by 5–10% with respect to the standard parametrization.

E_{OS} may be approximated by the molecular ionization potential for small molecules or as the energy of the highest occupied molecular orbital (HOMO), since the interacting electrons are peripheral ones and hence are roughly at the HOMO energy level. A more refined approach considers each pixel as a separate oscillator, with a formal ionization potential I_i , which in turn is a function of the ionization potential, I° , pertaining to the atom to whose basin the pixel belongs, and of the distance between the pixel and the atomic nucleus, R_i :

$$E_{\text{OS}} = (I_i)^{1/2}$$

$$I_i = I^\circ \exp(-\beta R_i)$$

The parameter β is a function of the atom type. This “variable-ionization” form of the theory amounts, in fact, to using different dispersion energy coefficients according to the different kinds of interacting atomic basins, and yields more accurate lattice energies in organic crystals.⁸

PIXEL calculations were applied to obtain separate Coulombic, polarization, dispersion, and repulsion contributions to the lattice energies, except for very large molecules, where the calculation of electron densities is too expensive, or for crystal structures with more than one molecule in the asymmetric unit, due to a technical difficulty with the evaluation of polarization contributions. For crystal structures in polar space groups, when the angle between the molecular dipole direction and a polar axis is small, a convergence correction should be applied to the lattice sums using the van Eijck–Kroon method;¹² for the very few cases when they were needed, however, these corrections were around 1–2 kJ mol⁻¹, so they were considered to be within the computational noise and were neglected. More information on separate driving forces in crystal packing (the “structure determinant” packing analysis) was then obtained from PIXEL interaction energies between near-neighbor pairs of molecules in the crystal.

IV. Results and Discussion

1. Density Distribution Functions and Packing Efficiency.

Figure 1 shows that in the database of nitro-derivative crystal structures, the oxygen–oxygen intermolecular distance distribution function (DDF) shows a well-developed peak at about $R(\text{O}\cdots\text{O}) = 3.2 \text{ \AA}$, a peak that does not appear when the same survey is conducted on a sample of $\sim 30\,000$ general organic crystals. We initially interpreted this unexpected fact as meaning that, due to the relevant Coulombic interactions present in these crystals, particularly those due to stabilizing interaction between nitro-nitrogen sites and nitro-oxygen sites, the peripheral oxygen atoms are forced into a close intermolecular contact that is counterintuitive in terms of simple atom–atom Coulombic interactions. The explanation actually requires a subtler analysis including penetration energies, i.e., those attractive energies which arise from overlap of diffuse electron clouds and their proximity to positively charged nuclei in the intermolecular partner.

A similar, but considerably smaller, peak is observed in the DDF of O \cdots H distances. This is not unexpected in view of the

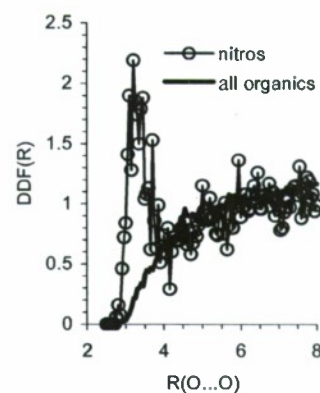


Figure 1. The density distribution function of O \cdots O separations in the sample of crystals of energetic materials of Table 1 (“nitros” line) and in a sample of 27 461 crystals of middle-size, general organic molecules containing only C, H, N, O, and halogen atoms, from the Cambridge Structural Database.

opposite sign of the molecular potentials around hydrogen atoms and oxygen atoms in nitro compounds, and a similar trend had been previously noted in a systematic study of nitrobenzenes.¹³ These results show the difficulty of defining intermolecular bonds in terms of short atom–atom intermolecular distances. Thus the postulate of existence of a C–H \cdots O crystal bond on the basis of atom–atom contacts alone requires explanation why the same analysis does not lead to the postulate of some kind of O \cdots O “bond” which would be in conflict with elementary chemical reasoning. Otherwise, supplementary reasoning must be produced for the distinction between the two cases, an alternative that is also not straightforward.

The energetic performance of materials is often related to high crystal density. This property stems from two unrelated factors: (a) molecular mass, or the number of protons and neutrons and (b) intermolecular close packing, related to electronic interactions. Overall,¹⁴ crystal density is determined mainly by molecular mass, an obvious property. For the design of materials for better transmission of heat and mechanical energy, factor b above, control of the relative efficiency by which space is occupied by constituent molecules of identical stoichiometry, is more challenging. A comparison between the packing coefficients¹⁵ for the present database and for a sample of general organic crystals (Figure 2), in spite of the large difference in statistical significance due to the large difference in sample size, is convincing in this respect. This observation is undoubtedly related to the relatively low number of hydrogen atoms in these molecules, which permits a higher interaction-energy density and parallels the previous observation of an unusual distribution of short contacts between peripheral oxygen atoms

2. Lattice Energies. An extensive set of lattice energy calculations using an empirical atom–atom force field for energetic materials with high quality ab initio atomic point charges has been carried out by Sorescu, Rice and Thompson (SRT).¹⁶ We use the lattice energy calculated by the universal UNI force field¹⁰ as a guideline, and Figure 3 plots the results obtained by the PIXEL scheme and by the SRT scheme, as well as the ΔH_{sub} . These data are collected in detail in Table 2. The best apparent agreement between experiment and calculation is that of the UNI potentials, with SRT potentials overestimating the lattice energies and PIXEL values showing an acceptable performance except for a few patent outliers (TNOXYL, TNIOAN, DATNBZ, HIHHAH, see also Table 2) where the calculated lattice energy is too small. One should recall, however, that the comparison is hampered on the one hand by

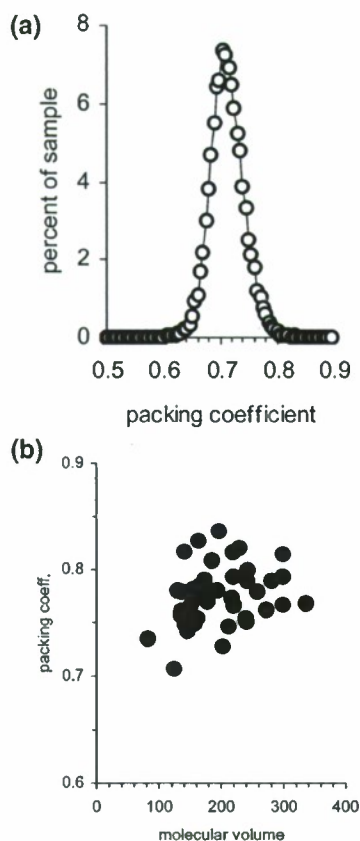


Figure 2. (a) Histogram of the percent distribution of packing coefficients in the general sample (see caption to Figure 1). The peak value is 0.70. (b) The distribution of the packing coefficients in the sample of crystals of energetic materials of Table 1 with average value of 0.77.

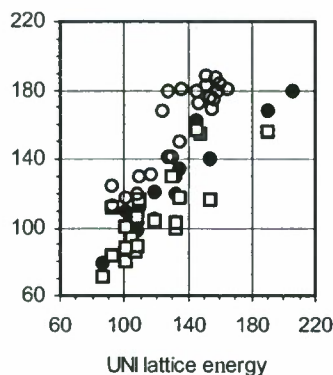


Figure 3. The UNI force-field lattice energy is the abscissa: on the ordinate are the sublimation enthalpies (black dots), the PIXEL lattice energies (squares), and the SRT lattice energies (circles); see Table 2 for the definitions. Units in kJ mol^{-1} .

the uncertainties of experimental values, as previously discussed, and, on the other hand, by the neglect of intramolecular rearrangement energies on going from the crystal to the gas-phase conformation. Accordingly, the overestimation of rigid-body lattice energies might be reasonable, where the correct sublimation enthalpy results after subtraction of the intramolecular energies.

The issue of accurate reproduction of experimental thermochemical data is complex, as previously discussed, but we argue that the added value of the PIXEL method consists in the energy partitioning (Table 2), which offers some insight into the nature of the energetic texture of crystalline materials not apparent in atom-atom schemes. PIXEL Coulombic energies are parameter-

free and are as accurate as the wavefunction is, while PIXEL dispersion energies depend, to some extent, on the parametrization. However, since Coulombic energies are exact and total lattice energies are quite comparable to experimental heats of sublimation, the dispersion contribution cannot be grossly off the mark. Therefore, the message in Table 2 is unequivocal: all lattice energies have a substantial Coulombic-polarization (what is commonly called "Coulombic") contribution, but dispersion energies are invariably equal to, or larger than, the Coulombic ones. This result, together with the previous analysis of oxygen-oxygen contacts, issues a warning against modeling schemes that rely too much on Coulombic energies, especially when they are estimated by atomic point-charge schemes, even for the compounds considered here that are commonly thought to possess a strong permanent polarization of their electron clouds.

3. Recognition Modes. Significant, further information on packing modes and packing forces in organic crystals comes from a calculation of interaction energies between pairs of close neighbor molecules in the PIXEL approach, the "structure determinant" analysis.¹⁷ To do this, one reference molecule is chosen and crystal symmetry is used to generate those molecules whose centers of mass are closest to the center-of-mass of the reference molecule. Then, each of these coordinated molecules is designated by (i) the distance between its center-of-mass and the reference molecule, (ii) the label of the symmetry operation connecting the two molecules, and (iii) the molecule-molecule interaction energy calculated by PIXEL and apportioned according to its various contributions: Coulombic, dispersion, and repulsion. A set of these geometrical and energetic values for a molecule pair is referred to as a "structure determinant," and a set of structure determinants is an unequivocal and accurate fingerprint of a crystal structure.

Data from this procedure are more informative than overall lattice energies because the PIXEL energy partitioning quantitatively clarifies the relative importance of Coulombic and dispersion terms, and establishes a more immediate correlation between packing forces and molecular electronic structure. Table 3 collects these lists for three representative crystals, and Figures 4-6 show the corresponding structural diagrams.

In the methyl nitramine crystal, the two determinants along the screw axis, *A* and *C*, roughly correspond to antiparallel nitro groups, but an interpretation based only on opposing dipoles is not warranted, given that the Coulombic and dispersion contributions are roughly equivalent. The nitro-methyl *B* determinant has a predominant Coulombic character. The next three determinants complete the first coordination shell made of 12 nearest-neighbors as in the close packing of spheroids (recall that each *S* or *T* interaction has two partners to the reference molecule). They are rather weak and sometimes have a destabilizing Coulombic component, like the *E* interaction which presents a confrontation of methyl groups, but are stabilized by a counterbalancing dispersion term.

In the CTMTNA crystal, the strongest binding comes from an interaction over a centrosymmetric molecular pair with the nitro-oxygens in one partner pointing to the nitro-nitrogen in the other. Here the Coulombic term is strongly stabilizing, as revealed by the PIXEL calculation, in spite of the unavoidable proximity of oxygen atoms. Notice, however, that in this case, too, the predominating factor is dispersion. It would have been quite difficult to properly describe this dominating interaction in pure atom-atom terms, and only the PIXEL description is adequate. The next determinant, *B*, is a clear $\text{O}\cdots\text{H}$ Coulombic interaction. However, it becomes increasingly difficult to assign

TABLE 3: Structure Determinants

determinant label,	$R(\text{c.o.m.}),$						approximate
	symmetry ^a	E_{coul}^b	E_{pol}	E_{disp}	E_{rep}	E_{tot}	description
METNAM							
A	3.86 S	-17	-3	-16	+7	-29	nitronitro antiparallel
B	6.13 T_z	-18	-4	-9	+9	-21	nitro-methyl, double
C	5.36 S	-10	-3	-10	+6	-16	nitronitro antiparallel, offset
D	6.58 T_x	-3	-1	-5	+3	-7	nitro-methyl, single
E	5.75 S	+3	-1	-10	+3	-5	methylmethyl offset
F	6.07 T_{xz}	+4	-1	-8	+3	-1	nonspecific
CTMTNA							
A	4.41 I	-17	-5	-38	33	-28	nitro cups
B	7.29 G_y	-18	-5	-17	14	-26	nitro-methylene
C	7.29 S_z	-17	-3	-12	7	-25	adjacent cups
D	6.94 G_x	-8	-4	-16	13	-15	oxygen-nitrogen
E	6.55 S_y	-6	-2	-10	6	-12	nonspecific dispersion
F	6.45 G_z	-5	-4	-23	19	-12	nonspecific dispersion
HMX							
βA	6.54 T_x	-37	-11	-36	29	-55	nested contact
αA	5.91 T_z	-41	-11	-27	29	-51	triple O...H contacts
βC	7.76 S	-13	-4	-20	13	-24	nonspecific
βB	7.37 T_{xz}	-10	-5	-20	12	-23	side contact
βD	7.03 S	-11	-4	-18	15	-17	single O...H contact
αB	8.13 G	-9	-5	-23	24	-13	nonspecific dispersion
αC	7.22 -	+2	-7	-23	19	-10	nonspecific dispersion
βE	10.9 T_{xz}	+5	-1	-3	1	+2	destabilizing

^a Label as in Figures 4–6, distance between centers of mass (com) (\AA); label of the symmetry operator: S = twofold screw, T = translation, I = inversion center, G = glide plane. ^b PIXEL partitioned energies and total molecule–molecule energy, kJ mol^{-1} .

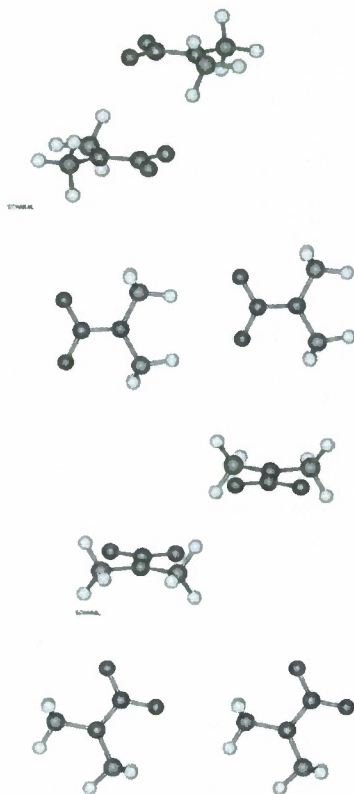


Figure 4. The structure determinants in the N,N-dimethylnitramine (METNAM) crystal structure. Top to bottom: A, B, C, and D (same labels as in Table 3).

an unequivocal label to the subsequent determinants, which comprise broad and diffuse mixtures of Coulombic and dispersion terms. The presence of these nonspecific structure deter-

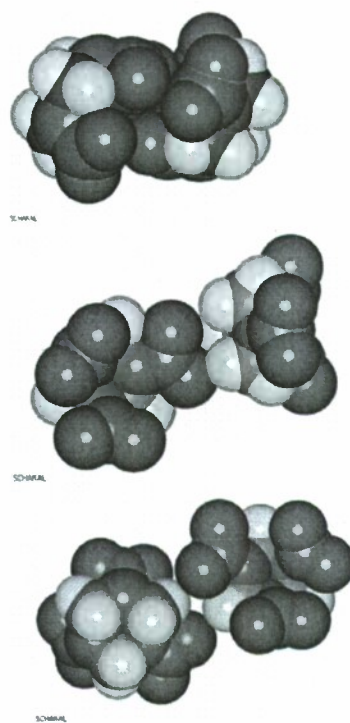


Figure 5. The structure determinants in the cyclotrimethylene-trinitramine (CTMTNA) crystal structure. Top to bottom: A, B, and C (same labels as in Table 3). Dark caps, nitro groups; white caps, hydrogen atoms.

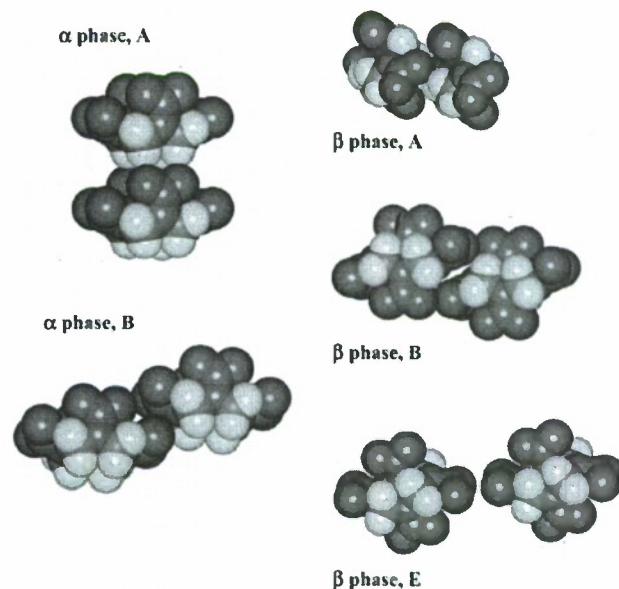


Figure 6. The structure determinants in the α phase HMX (OCHTET00) and β phase HMX (OCHTET12). Same labels as in Table 3. Dark caps, nitro groups; white caps, hydrogen atoms.

minants is what makes crystal-structure analysis, not to mention prediction and control, so difficult in terms of intermolecular atom–atom bonding.

The same analysis on the *A* and *D* molecular pairs in the CTMTNA crystal has been carried out¹⁸ with a methodology that in many respects resembles the PIXEL approach, using a HF/6-311G** wavefunction. The use of HF instead of MP2 leads to higher Coulombic energies, as is well-known. On the other hand, a comparison between the results of the two methods at the same wavefunction level (HF) gives very close values

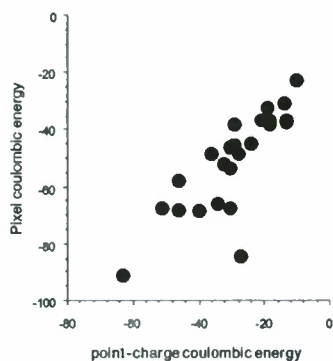


Figure 7. PIXEL exact Coulombic energy vs approximate point-charge Coulombic energy for the crystal structures listed in Table 2. kJ mol^{-1} units.

for the Coulombic + polarization term (-35.2 and -16.8 , PIXEL, -37.2 and -18.8 , ref 18).

The case with HMX is even more complex. Notice how the same molecule in two largely different conformations can build up crystal structure determinants of nearly equal intensity in two polymorphic crystals: the α form by a clear confrontation of its nitro and methylene moieties with Coulombic stabilization (αA determinant), and the β form by a less clear-cut “nested” contact (βA determinant), with an equal amount of Coulombic and dispersive character. In the β form, a near-neighbor pair (βE) displays a sharp confrontation of opposing nitro groups where the distance prevents an overlap of the molecular electron densities and no penetration energy sets in. The resulting Coulombic interaction energy is mildly destabilizing, but a minor amount of dispersion from the overall molecular bodies is more than enough to wipe out the repulsion. Thus, the PIXEL analysis reveals the presence of nonspecific stabilizing or even “silent”, slightly destabilizing partners whose role in crystal packing is difficult to assess but is by no means negligible, although they are usually neglected in standard crystal packing analyses based on short interatomic distances only.

4. Point-Charge versus PIXEL Coulombic Energies. A comparison between PIXEL Coulombic lattice energies and point-charge Coulombic energies is instructive. Figure 7 shows the result: the good news is that there is a rather consistent proportionality ratio by which the point-charge energy is about 60% of the real Coulombic energy. This could be useful in the rescaling of empirical, force-field parametrizations. There are, however, some patent outliers where the point-charge model is severely off the mark. The case of triamino-trinitrobenzene, with its extensive hydrogen-bonding network, is exemplary in this respect.

V. Conclusions

The quantitative analysis of structures and interaction energies in crystals of energetic compounds is in many respects revealing. With their high number of nitro groups, these molecules have a low relative abundance of hydrogen atoms and in their crystals they must make do with an unusually high number of contacts between peripheral oxygen atoms. These are indeed numerous and anomalously short, as clearly appears in a quantitative study based on the newly introduced concept of Density Distribution Functions (DDF's). Packing coefficient values are unusually high, most likely as a consequence of a higher interaction energy density. Calculated lattice energies compare rather favorably with experimental sublimation enthalpies in all of the computational schemes employed here. The comparison is, however, much less compelling than is usually thought in molecular

simulation and force-field calibrations because of the large uncertainties in experimental values and because of the many approximations, especially the rigid-molecule approximation, which is particularly restrictive for many of the compounds examined here. The PIXEL analysis has an average performance in regard to total lattice energies but is superior in its interpretative power because it is based on complete electron distributions rather than on a few, localized, interaction centers. The PIXEL analysis reveals that (i) short oxygen–oxygen separations do not imply repulsive or destabilizing interactions, a probable conclusion arising from a superficial analysis in terms of atom–atom contacts, and (ii) dispersive contributions to the interaction energies are invariably higher, contrary to common belief.

The studies presented here use molecular simulations based on a perfect model, an infinite, homogeneous crystal without defects. Whether this model is adequate or not depends on which crystal properties are studied. We suggest that our results are significant concerning the general conclusions regarding structural features of these crystals: atom–atom distance distributions and packing coefficients, and the general nature of the crystal packing forces, especially their subdivision into Coulombic and dispersive components.

In any case, simulation of perfect crystals is expected to provide a paradigm by which the effect of imperfections can be discussed. Moreover, molecule–molecule interaction energies do not depend on a global model of the bulk crystal and are therefore certainly informative and reliable. A proper consideration of the role of defects will certainly be needed when tackling a molecular simulation for a more detailed investigation of subtle factors which determine the properties related to reactivity, decomposition and mass or heat transport of these materials. This is left for future work.

Acknowledgment. This collaboration was made possible by a faculty development leave from the University of Nebraska-Lincoln awarded to CJE. The research was supported, in part, by the US Office of Naval Research under Grant No. N00014-06-1-0265 (CJE). The molecular diagrams were drawn with the help of the SCHAKAL program.¹⁹

Supporting Information Available: Atomic coordinate files, including renormalized hydrogen atom positions, for all the crystal structures considered. This information is available free of charge via the Internet at <http://pubs.acs.org>.

References and Notes

- (1) (a) Freid, L. E.; Manaa, M. R.; Pagoria, P. F.; Simpson, R. L. *Annu. Rev. Mater. Res.* **2001**, *31*, 291–321. (b) Borne, L.; Patedoye, J.-C.; Spycerelle, C. *Propellants Explos. Pyrotechn.* **1999**, *24*, 255–259.
- (2) Lothrop, W. C.; Handrie, G. R. *Chem. Rev.* **1949**, *44*, 419–445.
- (3) (a) Hatano, T. *Phys. Rev. Lett.* **2004**, *92*, 085501/1–4. (b) van der Heijden, A. E. D. M.; Bouma, R. H. B. *Cryst. Growth Des.* **2004**, *4*, 999–1007. (c) Armstrong, R. W.; Ammon, H. L.; Elban, W. L.; Tsai, D. H. *Thermochem. Acta* **2002**, *384*, 303–313. (d) Kuklja, M. M.; Kunz, B. A. *J. Phys. Chem.* **1999**, *B103*, 8427–8431.
- (4) Gavezzotti, A. *Molecular Aggregation*; Oxford University Press, Oxford, 2006. Computer codes for the software used in this paper and reference manuals can be downloaded from <http://users.unimi.it/gavezzot> as supplementary material to the book.
- (5) Afeefy, H. Y.; Liebman, J. F.; Stein, S. E. Neutral Thermochemical Data. In *NIST Chemistry WebBook*; NIST Standard Reference Database Number 69; Linstrom, P. J., Mallard, W. G., Eds.; National Institute of Standards and Technology: Gaithersburg, MD, 2003 (<http://webbook.nist.gov/chemistry>). Chickos, J. S. Heat of Sublimation Data. In *NIST Chemistry WebBook*; NIST Standard Reference Database Number 69; Linstrom, P. J., Mallard, W. G., Eds.; National Institute of Standards and Technology: Gaithersburg, MD, 2003 (<http://webbook.nist.gov/chemistry>).
- (6) (a) Cundall, R. B.; Palmer, T. F.; Wood, C. E. C. *J. Chem. Soc., Faraday Trans. 1* **1978**, *43*, 1339–1345. (b) Lyman, J. L.; Liao, Y.-C.;

Brand, H. V. *Combust. Flame* **2002**, *130*, 185–203. (c) Taylor, J. W.; Crookes, R. J. *Combust. Flame* **1973**, *21*, 391–393.

(7) Allen, F. H.; Kennard, O. *Chem. Des. Automation News* **1993**, *8*, 31–37.

(8) See ref 4, Chapter 12.

(9) Frisch, M. J.; Trucks, G. W.; Schlegel, H. B.; Scuseria, G. E.; Robb, M. A.; Cheeseman, J. R.; Montgomery, J. A., Jr.; Vreven, T.; Kudin, K. N.; Burant, J. C.; Millam, J. M.; Iyengar, S. S.; Tomasi, J.; Barone, V.; Mennucci, B.; Cossi, M.; Scalmani, G.; Rega, N.; Petersson, G. A.; Nakatsuji, H.; Hada, M.; Ehara, M.; Toyota, K.; Fukuda, R.; Hasegawa, J.; Ishida, M.; Nakajima, T.; Honda, Y.; Kitao, O.; Nakai, H.; Kiene, M.; Li, X.; Knox, J. E.; Hratchian, H. P.; Cross, J. B.; Adamo, C.; Jaramillo, J.; Gomperts, R.; Stratmann, R. E.; Yazyev, O.; Austin, A. J.; Cammi, R.; Pomelli, C.; Ochterski, J. W.; Ayala, P. Y.; Morokuma, K.; Voth, G. A.; Salvador, P.; Dannenberg, J. J.; Zakrzewski, V. G.; Dapprich, S.; Daniels, A. D.; Strain, M. C.; Farkas, O.; Malick, D. K.; Rabuck, A. D.; Raghavachari, K.; Foresman, J. B.; Ortiz, J. V.; Cui, Q.; Baboul, A. G.; Clifford, S.; Cioslowski, J.; Stefanov, B. B.; Liu, G.; Liashenko, A.; Piskorz, P.; Komaromi, I.; Martin, R. L.; Fox, D. J.; Keith, T.; Al-Laham, M. A.; Peng, C. Y.; Nanayakkara, A.; Challacombe, M.; Gill, P. M. W.; Johnson, B.; Chen, W.; Wong, M. W.; Gonzalez, C.; Pople, J. A. *Gaussian 03*, Revision A.1; Gaussian, Inc.: Pittsburgh, PA, 2003.

(10) Gavezzotti, A.; Filippini, G. *J. Phys. Chem.* **1994**, *98*, 4831–4837.

(11) (a) Gavezzotti, A. *J. Phys. Chem. B* **2002**, *106*, 4145–4154. (b) Gavezzotti, A. *J. Phys. Chem. B* **2003**, *107*, 2344–2353. (c) Gavezzotti, A. *J. Chem. Theor. Comp.* **2005**, *1*, 834–840. See ref 5, Chapter 12, for more details.

(12) van Eijck, B. P.; Kroon, J. *J. Phys. Chem.* **1997**, *B101*, 1096–1100.

(13) Demartin, F.; Filippini, G.; Gavezzotti, A.; Rizzato, S. *Acta Crystallogr., Sect. B* **2004**, *60*, 609–620.

(14) Dunitz, J. D.; Filippini, G.; Gavezzotti, A. *Tetrahedron* **2000**, *56*, 6595–6601.

(15) The packing coefficient is defined as the ratio of molecular volume to cell volume. These were calculated by numerical integration rather than by the Kitaigorodski spheres-and caps method (Kitaigorodski, A. I. *Organic Chemical Crystallography*, Consultants Bureau, New York 1961) which is rather inaccurate for molecules with nitro groups.

(16) Sorescu, D. C.; Rice, B. M.; Thompson, D. L. *J. Phys. Chem. A* **1998**, *102*, 8386–8392.

(17) Gavezzotti, A.; Filippini, G. *J. Am. Chem. Soc.* **1995**, *117*, 12299–12305.

(18) Politzer, P.; Ma, Y. *Int. J. Quantum Chem.* **2004**, *100*, 733–739.

(19) Keller, E. *SCHAKAL92, A Program for the Graphic Representation of Molecular and Crystallographic Models*; University of Freiburg: Freiburg, 1993.